Surface & Coatings Technology 205 (2010) 1979–1984

Contents lists available at ScienceDirect

Surface & Coatings Technology

journal homepage: www.elsevier.com/locate/surfcoat

# Characteristics of Ni–Ir and Pt–Ir hard coatings surface treated by pulsed Nd:YAG laser

Shih-Feng Tseng [a,b,*], Wen-Tse Hsiao [a], Kuo-Cheng Huang [a], Ming-Fei Chen [c], Chao-Te Lee [a], Chang-Pin Chou [b]

[a] Instrument Technology Research Center, National Applied Research Laboratories, Hsinchu 30076, Taiwan
[b] Department of Mechanical Engineering, National Chiao Tung University, Hsinchu 30010, Taiwan
[c] Department of Mechatronics Engineering, National Changhua University of Education, Changhua 50007, Taiwan

ARTICLE INFO

*Article history:*
Received 1 March 2010
Accepted in revised form 19 August 2010
Available online 24 August 2010

*Keywords:*
Laser surface treatment
Protective coatings
Ion source assisted magnetron sputtering system
Nd:YAG laser

ABSTRACT

The subjects of the presented paper are to develop a laser surface treatment technology for the protective coatings of glass-molding dies and to better understand the interaction between laser beam and materials coated on the die surface. A variety of alloy films, including Ir-25 at.% Pt, Ir-50 at.% Pt, Ir-75 at.% Pt, Ir-25 at.% Ni, Ir-50 at.% Ni, and Ir-75 at.% Ni compositions are deposited by the ion source assisted magnetron sputtering system (ISAMSS). A Cr layer that functioned as a buffer layer is deposited between the alloy film and die surface. After an alloy film and the buffer Cr layer were sequentially coated on tungsten carbide (WC) surface, Nd:YAG laser was directly applied in the writing process. The temperature profile of the film stack structure is simulated by ANSYS software. The surface roughness was analyzed by atomic force microscopy (AFM) to compare the coating surface roughness before and after the laser surface treatments. The treated coatings for oxidation prevention test were examined by energy dispersive x-ray spectrometry (EDS). Nanoindentation instrument was performed to evaluate microhardness and reduced modulus of the coatings. The cross-sectional structures between the hard coating layer and buffer layer were also inspected by a scanning electron microscope (SEM). The Pt–Ir and Ni–Ir film coatings are unable to withstand the working temperature over 1500 °C, which is considered for quartz molding process and hot embossing process. The films showed high roughness, low microhardness and low reduced modulus because the film oxidation occurred in a high working temperature process.



## 1. Introduction

Glass materials have excellent optical properties, such as a high refractive index and low optical energy absorption in a visible light spectrum, and high chemical and heat resistance, and are one of important materials used in the variety of key components and devices. Glass materials are much more suitable than plastic materials applied for high temperature, humid or harsh environments. For those reasons, glass lenses are dominantly used in opto-electronic and biomedical devices. Low cost and high performance glass lenses are mostly produced by high precision molding technology. Consequently, the protective films are necessary for the glass-molding dies to resist elevated temperature and pressure. The protective films of different chemical compositions and processes are developed to satisfy the different glass operated conditions and to improve and extend the molding die lifetime.

Tungsten carbide (WC) was used as the mold material in the glass-molding process. This material is very hard and brittle but offers good performance in glass-molding dies. Pt–Ir, CrN, CrWN, and Mo–Ru thin films are reported to coat the mold surface and to increase the lifetime of molds. Tseng et al. [1] discussed the mechanical properties of Pt–Ir and Ni–Ir binary alloys for the glass-molding die coating. With increasing Pt and Ni doping contents in Ir-based coatings, the microhardness of both coatings decreased significantly and the values of the reduced modulus of Pt–Ir alloys are larger than that of Ni–Ir alloys. After the oxidation testing of these Ir-based coatings exposed at 700 °C by a glass-molding machine, the oxygen concentration in Pt–Ir coatings does not obviously change with increasing Pt contents. However, the oxygen concentration of Ni–Ir coatings shows large variations even though the glass-molding operation was conducted under the $N_2$ atmosphere. Lin et al. [2] proposed CrWN coatings with the tungsten contents of 0 23.4 at.% coated on WC substrates by ion beam assisted deposition. With 4.4 at.%, 7.1 at.%, 13.1 at.%., and 19.7 at.% tungsten doping contents in CrN coatings, the smooth surfaces were obtained and surface roughness Ra is less than 2 nm. After oxidation test at 750 °C in air atmosphere, the $Cr_2O_3$ precipitates were formed and resulted in the large roughness of more than 40 nm on the CrN and CrWN coating surface. However, the CrWN coatings with 4.4 at.% to 16.7 at.% tungsten contents revealed smooth surface and improved hardness that can be applied in glass-molding

* Corresponding author. Instrument Technology Research Center, National Applied Research Laboratories, Hsinchu 30076, Taiwan. Tel.: +886 3 5779911x227; fax: +886 3 5773947.
*E-mail address:* tsengsf@itrc.narl.org.tw (S.-F. Tseng).

0257-8972/$ – see front matter. Crown Copyright © 2010 Published by Elsevier B.V. All rights reserved.
doi:10.1016/j.surfcoat.2010.08.075

die coatings. The Mo–Ru binary alloys with Cr and Ti twin buffer layers deposited on WC substrates as the protective coatings were investigated [3,4]. With the higher Ru doping contents in Mo-based coatings, the results show that the Mo–Ru alloys have better oxidation resistance but also have a higher surface roughness. Moreover, Wei and Shieh [5] proposed the TaN binary compounds and $Ta_{1-x}W_xN_y$ ternary compounds deposited on the WC dies and silicon wafers by ion beam sputtering. The $Ta_{1-x}W_xN_y$ films reveal better high temperature performance than the TaN films for glass-molding die coatings such as high melting point, high hardness, and chemical resistance. These films are anti-adhesive and have excellent chemical stability and good coating stability under working environment. Moreover, laser surface treatment can improve the toughness and durability of film materials to further enhance the performance of the mold surface.

Rosenthal [6] proposed a mathematic model to thermally evaluate the transient temperature field of working pieces for point, line, and surface heating laser sources. Kang et al. [7] applied a finite element program ABAQUS to analyze the heat transfer and residual distortion for laser welding LD (laser diode) pump on EDFA (erbium doped fiber amplifier). In the Nd:YAG laser welding process, distortion occurs at the ferrule and saddle during the heating and cooling processes of welding. Gordon et al. [8] provided a simulation tool for a laser manufacturing process. He discussed the relationship between pulse energy, etch rate, pulse frequency and the preheating temperature of the substrates. Laser processing is another surface heat treatment that usually provides the advantages of no contact between the tools and work specimens, high temperature, lack of tool wear, high speed, and few thermal effects [9]. Liu et al. [10] discussed a pulse laser-textured method that uses a Co-based WC–TiC sintered carbide coating. They also investigated the resulting microstructure, roughness, hardness, and wear resistant properties of coatings. Textured surfaces have many advantages and the most important one is to improve mechanical performance, such as surface hardness [11], tribological behaviour [12], and lubricating of friction [13,14]. Wan [15] proposed a novel laser coating and texturing technique to improve surface topographies and friction behaviour. Tseng [16] reported a surface-texturing technique to create rough patterns on a silicon substrate and to investigate the wettability on a laser-textured surface.

In the glass-molding or in the glass hot embossing process, a preform glass is heated 20 °C to 40 °C above its yield point and pressed in a pumped nitrogen gas atmosphere. The working temperatures are approximately 500 °C for glasses such as P-SK57, N-PK51, L-LAM69, which are usually used in most molding applications with a low transformation temperature ($T_g$). However, the fused silica has a high $T_g$ point, and must be heated to 1400 °C–1500 °C before pressed. This study aims to found an operation environment of the glass-molding process by laser irradiations and to investigate the interaction between a laser beam and protective coatings under an ambient atmosphere and a temperature of 1500 °C. The tungsten carbide mold was made of FUJI J05 type material with a diameter of 10 mm and a thickness of 5 mm. Pt–Ir and Ni–Ir alloy films were deposited by an ion source assisted magnetron sputtering system (ISAMSS). A variety of Ir-based compositions, including 25 at.% Pt, 50 at.% Pt, 75 at.% Pt, 25 at.% Ni, 50 at.% Ni and 75 at.% Ni were used. A commercial finite element analysis (FEA) software was used to simulate the temperature profile of these Ir-based alloy films irradiated by pulsed Nd:YAG laser because the temperature generated by pulsed laser is difficult to monitor by practical measured methods. The pulsed laser treatment technique has many advantages such as fast, energy-saving, and novel excelling over other traditional furnace treatment. In addition, the properties such as surface roughness, morphology, oxidation, microhardness and reduced modulus are also discussed. Finally, the simulation results and experimental results are compared.

## 2. Experimental

### 2.1. Numerical simulation process

Finite element analysis is a powerful tool for engineering prediction of material characteristics and manufacturing process parameters. We conduct thermal analysis on a FUJI J05 WC mold with Ir-based coatings treated by the laser using ANSYS software. The physical properties of the WC mold shown in Table 1 were used to evaluate temperature distribution. Because the single-pulse exposure time is very short on the material surface during laser heating, the effects of convection and radiation were ignored in our simulation conditions. Some assumptions made are shown in the following:

(1) The thermal properties of all analyzed materials are isotropic.
(2) Laser beam intensity distribution is a $TEM_{00}$ mode.
(3) Any phase change phenomena is ignored in the heating process.
(4) The heat conduction and thermal radiation are ignored in the parameter setting.

The finite element model was applied to analyze the temperature distribution of the WC molds with 10 mm in diameter and 5 mm thick. The mold samples were coated with different compositions of Pt–Ir and Ni–Ir alloys. The optical absorption parameters of specimens, including Ir-25 at.% Pt, Ir-50 at.% Pt, Ir-75 at.% Pt, Ir-25 at.% Ni, Ir-50 at.% Ni, and Ir-75 at.% Ni, were respectively calculated using ANSYS software for the mathematical model and temperature distribution.

There are three analysis steps proceeded in ANSYS software: (1) pre-processing (2) solution processing (3) post-processing. The pre-processing includes modeling and meshing processes. To set up the thermal properties in the modeling process, the input parameters consist of density, thermal conductivity and specific heat of the WC mold substrate as shown in Table 1. The diameter and thickness of the WC mold were defined as 10 mm and 5 mm, respectively. Moreover, the grid size of the element unit was set 20 μm during the meshing process. The boundary conditions for solution processing include the load of the material, initial temperature, and laser parameters. The initial temperature was 27 °C, the pulse repetition frequency was fixed at 100 kHz, the single-pulse exposure time was 100 μs, and a function-editor was employed to define the Gaussian heat source in our simulation condition. In the simulation processing, the surface temperature was approximately 1500 °C; hence, the average power levels were adjusted to approach the high surface temperature of various Pt–Ir and Ni–Ir alloys thin films, depending on the absorption characteristics of the film alloys.

### 2.2. Laser surface treatment system

Fig. 1 depicts the experimental system. The system consisted of a Nd:YAG laser, a beam delivery system, a focusing lens, and a PC-based controller. The Nd:YAG laser used in this study is a fundamental laser generator produced by Aptowave Corporation with a wavelength of 1064 nm. The pulse repetition rate can be adjusted from 1 kHz to 100 kHz and the maximum laser output power is 20 W. The beam delivery system includes three prefect mirrors and a 5× magnification

**Table 1**
Physical characteristics of tungsten carbide (WC) mold for glass molding.

| Physical properties | FUJI J05 WC |
|---|---|
| Young modulus (GPa) | 650 |
| Poison ratio | 0.21 |
| Density ($kg/m^3$) | 14650 |
| Thermal conductivity (W/m °C ) | 63 |
| Coefficient of thermal expansion ($\times 10^{-6}$/°C) | 5.1 |
| Specific heat (J/kg °C) | 314 |

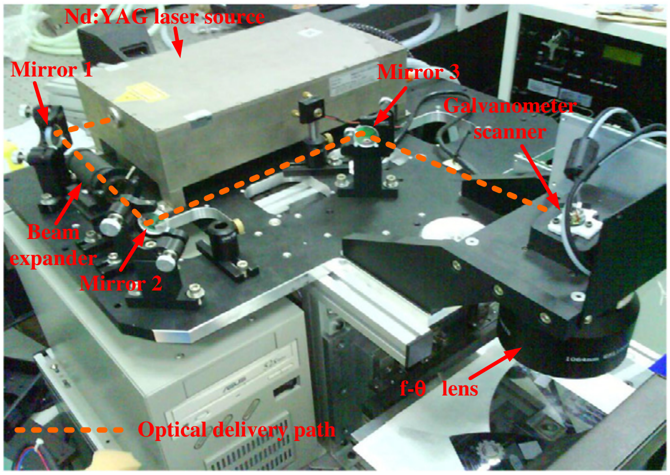


**Fig. 1.** The experimental setup of the Nd:YAG laser system.

beam expander. The z-axis feeding system can adjust the position of the laser focusing point. The working distance of the used focusing lens is of 134 mm and the minimum spot size is of about 15 μm focused in this Nd:YAG laser system.

### 2.3. Sample preparation

The Ni–Ir and Pt–Ir films of various compositions were deposited by an ion source assisted magnetron sputtering system (ISAMSS) on a substrate at a heated temperature of 400 °C. The RF powers of 100 W at Pt and Ni targets, and the tunable RF powers of 100–200 W and 100–300 W at the Ir target are operated, respectively. The deposition conditions are conducted under a vacuum environment of less than $5\times10^{-6}$ Torr, a working gas of argon, and a working pressure at 5 mTorr. All the Pt–Ir and Ni–Ir thin films were approximately 300 nm thick. To obtain better Pt–Ir and Ni–Ir alloy adhesion on the mold, a chromium (Cr) layer of 50 nm thickness was deposited on the WC mold surface to act as a buffer layer. An AFM (Veeco di Dimension 3100) was used to measure the film surface roughness of the Pt–Ir and Ni–Ir alloy thin films before and after laser surface treatment. A field emission scanning electron microscope (FESEM, Model JEOL JSM-7401F) with energy dispersive X-ray spectrometry (EDS) was used to observe the cross-sectional view and to analyze chemical composition of the films. The microhardness and reduced modulus of these films were measured with a nanoindentation tester (Hysitron TriboLab, USA) equipped with a Berkovich indenter.

## 3. Results and discussions

### 3.1. SEM observations on different composition alloy films

Fig. 2 shows the cross-section images of Pt–Ir and Ni–Ir alloy films deposited on a silicon substrate taken by a scanning electron microscope (SEM). Fig. 2(a) shows that the film layer of Ir-50 at.% Ni alloy was approximately 300 nm thick while the Cr buffer layer was approximately 58 nm thick. Fig. 2(b) shows that the film layers of Ir-50 at.% Pt alloy and Cr were approximately 306 nm and 51 nm thick, respectively. The clear and typical column crystallines of Pt–Ir and Ni–Ir coatings grown from the chromium buffer layer deposited on a silicon substrate are observed by SEM.

### 3.2. The temperature distribution profile of the different composition alloy films

First, spectrophotometry (Lambda 900) is used to determine the reflectance (R) of the WC substrate with different Ir-based

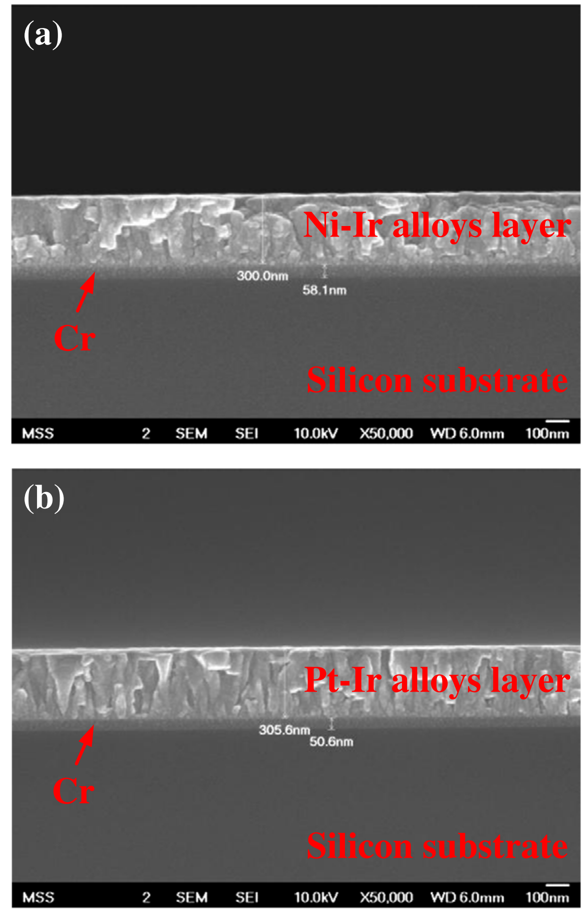


**Fig. 2.** Cross-section views of Ni–Ir and Pt–Ir films deposited on silicon substrates observed by SEM. (a) Ir-50 at.% Ni, (b) Ir-50 at.% Pt.

alloy coatings. Fig. 3 shows the reflectance spectra of different Pt–Ir and Ni–Ir alloy composition films. These results show that reflectivity in the Nd:YAG laser infrared spectrum (wavelength@1064 nm) is from 76% to 81% . Because the thin films were not transparent for the Nd:YAG laser wavelength, the absorptance (A) is calculated to be from 24% to 19% by substituting reflectance values into $A = 1-(R+T)$.

Fig. 4 displays a cross-section view of the temperature distribution on the WC substrate with Ir-25 at.% Ni coating after a 100 μs single-

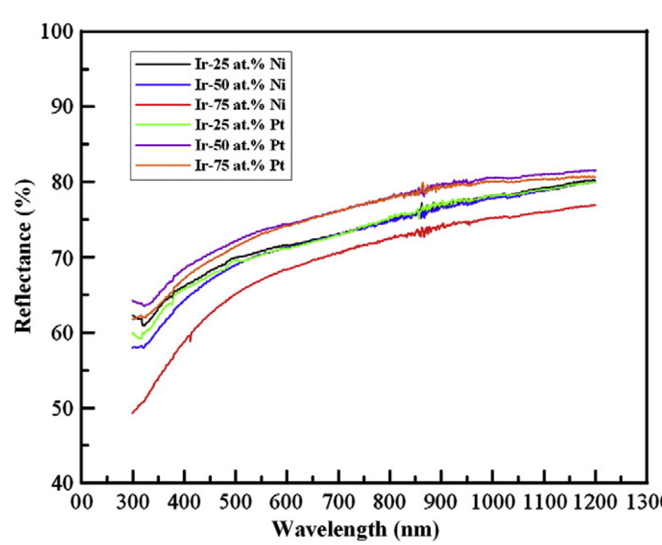


**Fig. 3.** Optical reflectance versus wavelength for different composition alloys.

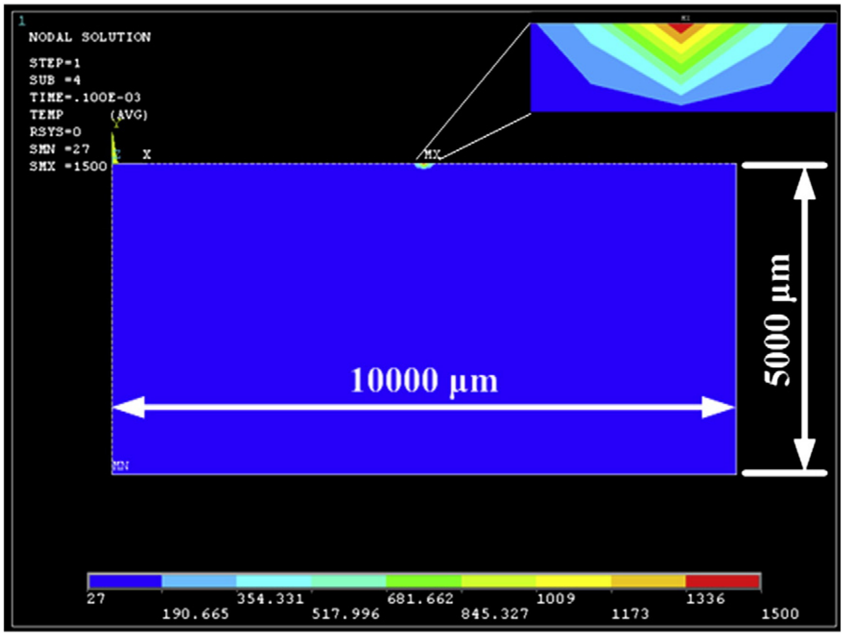


**Fig. 4.** A cross-section view of temperature distribution on WC mold with Ir-25 at.% Ni coating calculated by ANSYS simulation.

pulse exposure time, a pulse repetition frequency of 100 kHz and a laser output power level of 5.2 W. The initial temperature of irradiation was 27 °C and the maximum heating temperature was controlled at approximately 1500 °C. A series of the laser output power levels were calculated by ANSYS software to be 5.2 W, 5.13 W, 4.55 W, 5.07 W, 5.76 W and 5.58 W for Ir-25 at.% Ni, Ir-50 at.% Ni, Ir-75 at.% Ni, Ir-25 at.% Pt, Ir-50 at.% Pt, and Ir-75 at.% Pt, respectively. Hence, the processing parameter values of laser treatment calculated by ANSYS simulation are summarized in Table 2.

### *3.3. Description of surface roughness of Pt–Ir and Ni–Ir films treated by laser annealing*

All Pt–Ir and Ni–Ir thin films were deposited on WC molds by ion source assisted magnetron sputtering. Because the overlapping area of the sequential laser spot is over 99% during the laser treatment on these films, and we apply laser treatment on the whole film which is 10 mm diameter side. The AFM was used to measure the film surface roughness in the middle film surface. Table 3 shows the surface roughness of different alloy compositions before and after the laser treatments. Before the laser treatment, the surface roughness values $R_a$ ranged from 34.26 nm to 12.5 nm with a measuring region of $10 \times 10$ μm$^2$. The roughness increases dramatically up to 1-order high after the laser treatments. The geometric surface features of films after laser treatments are summarized in Fig. 5. Fig. 5 shows the surface roughness after laser treatment, clearly showing that the surface roughness increases over 100 nm. Moreover, the values of surface roughness are obviously increased as increasing concentrations of Pt or Ni. This trend is similar to the results reported in the glass-molding machine annealing on Pt–It and Ni–Ir coatings [1]. Furthermore, a comparison of different Ni–Ir alloy compositions versus the laser output power of treatment parameters indicates that a higher film surface absorption produced a greater surface roughness.

**Table 2**
Summarized table of processing parameters for laser treatment.

| Compositions | Absorptance @1064 nm | Single-pulse exposure time | Pulse repetition frequency (kHz) | Laser power (W) | Treatment temperature (°C) |
|---|---|---|---|---|---|
| Ir-25 at.% Ni | 21.28 | 100 | 100 | 5.2 | 1500 |
| Ir-50 at.% Ni | 21.59 | | | 5.13 | 1501 |
| Ir-75 at.% Ni | 24.33 | | | 4.55 | 1501 |
| Ir-25 at.% Pt | 21.38 | | | 5.07 | 1500 |
| Ir-50 at.% Pt | 19.21 | | | 5.76 | 1500 |
| Ir-75 at.% Pt | 19.82 | | | 5.58 | 1499 |

### *3.4. Oxidation analysis using EDS*

The oxide effect on the surface roughness is examined because surface roughness is an important parameter in the glass-molding process and the rough surface is resulted from oxide. In this research, the laser surface treatment of Pt–Ir and Ni–Ir alloys was conducted at room temperature without protection during laser irradiation. Fig. 6 shows the oxygen concentrations of Ir-based alloys measured by EDS after laser treatment. The oxygen concentration of Pt–Ir coatings is lower than that of Ni–Ir coatings, and the difference is approximately 3 to 5 at.% O. Moreover, the oxygen concentration of these alloys increases obviously with increasing Pt or Ni doping. For Ir-75 at.% Ni coatings, in particular, the deposited film was seriously oxidized and the roughness Ra value is the largest one among all Ir-based coatings subjected to the oxidation testing. Due to the serious oxidation, the thin film that contained 75 at.% Ni is unusable to be a protective coating applied on glass-molding dies. To investigate the anti-oxidation behaviour, these thin films are annealed at 700 °C under a nitrogen gas atmosphere using a glass-molding machine conducted by Tseng et al. [1]. However, the oxygen concentration of these films is greatly increased because the operation environment of this laser treatment is at the 1500 °C elevated temperature in the air and not filled with protective gas.

### *3.5. Microhardness and reduced modulus property*

Figs. 7 and 8 show the microhardness and reduced modulus test results measured by the Nanoindentation instrument, respectively. The microhardness and reduced modulus measurement procedure is introduced and each process including loading, holding, and unloading takes 5 s. An indentation depth of 30 nm ± 10% and a maximal loading of 50 μN were adopted in this study. The average

**Table 3**
Comparison of surface roughness before and after laser treatment.

| Compositions | Surface roughness (nm) | |
|---|---|---|
| | Before laser treatment | After laser treatment |
| Ir-25 at.% Ni | 12.50 | 137.71 |
| Ir-50 at.% Ni | 17.21 | 154.14 |
| Ir-75 at.% Ni | 34.26 | 189.09 |
| Ir-25 at.% Pt | 12.52 | 117.24 |
| Ir-50 at.% Pt | 14.92 | 157.09 |
| Ir-75 at.% Pt | 17.90 | 178.00 |

values with the standard deviation measured from five spots on each specimen were illustrated. After laser surface treatment at 1500 °C, the microhardness values of Ni–Ir and Pt–Ir coatings increased from 0.4812 to 0.824 GPa and from 0.79 to 1.5 GPa with decreasing concentrations of Ni and Pt, respectively. All the microhardness values of laser treated films are lower than the original ones. In addition, the reduced modulus values decreased from 31.89 to 15.02 GPa as the Pt concentrations decreased. Moreover, the Ir-25 at.% Ni of reduced modulus had a minimum value of 15.91 GPa. Due to the oxidation reaction between alloy materials and oxygen [17], these tested values of microhardness and reduced modulus of laser treated coatings apparently decreased than the un-treated ones.

## 4. Conclusion

The subjects of the presented paper are to develop a laser surface treatment technology for the protective coatings of glass-molding dies and to better understand the interaction between laser beam and materials coated on the die surface. After laser surface treatment at 1500 °C, the values of surface roughness are obviously increased as increasing concentrations of Pt or Ni. Moreover, the anti-oxide ability of Pt–Ir thin films has been validated to be better than Ni–Ir thin films. The Pt–Ir and Ni–Ir coatings are unable to withstand the working temperature over 1500 °C, which is considered for quartz molding process and hot embossing process. The surface films are high roughness, low microhardness and low reduced modulus because of the film oxidation that occurred in a high working

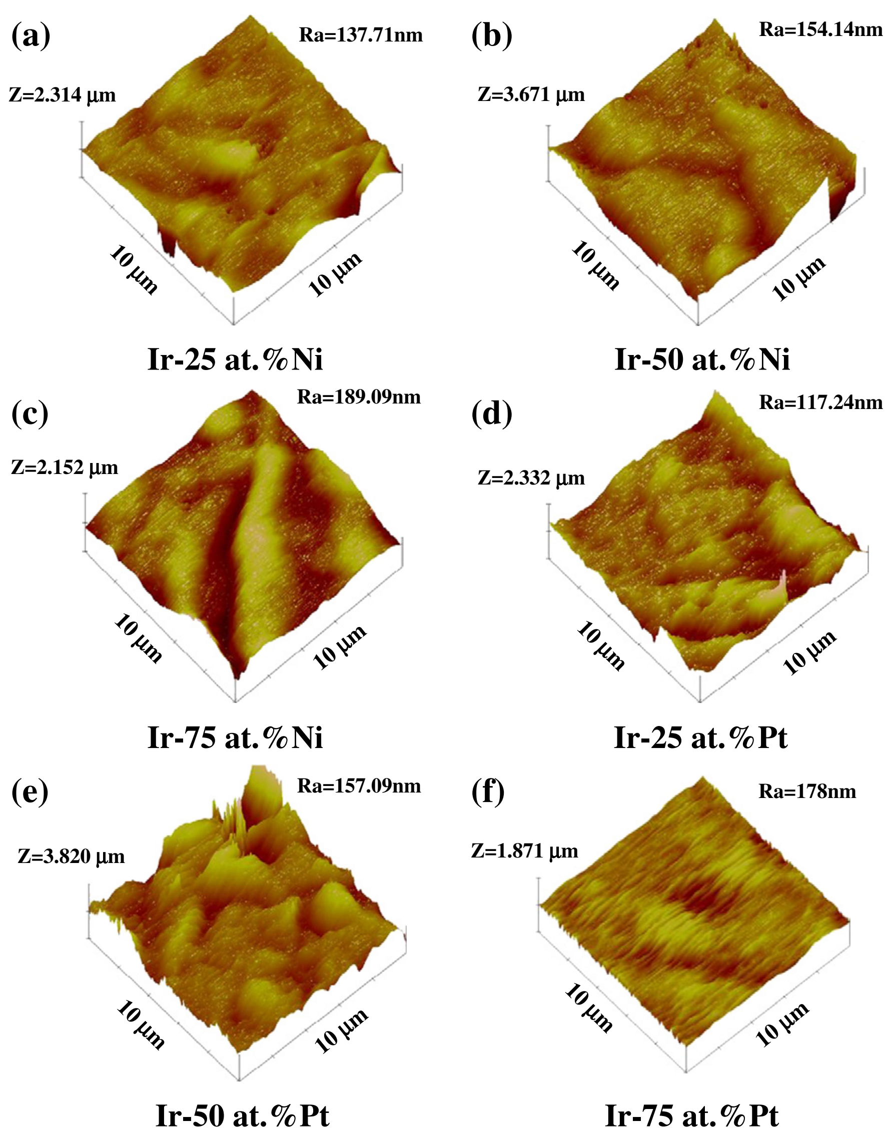


**Fig. 5.** Surface roughness of different alloy coatings after laser surface treatment. The coatings composition are (a) Ir-25 at.% Ni, (b) Ir-50 at.% Ni, (c) Ir-75 at.% Ni, (d) Ir-25 at.% Pt, (e) Ir-50 at.% Pt and (f) Ir-75 at.% Pt.

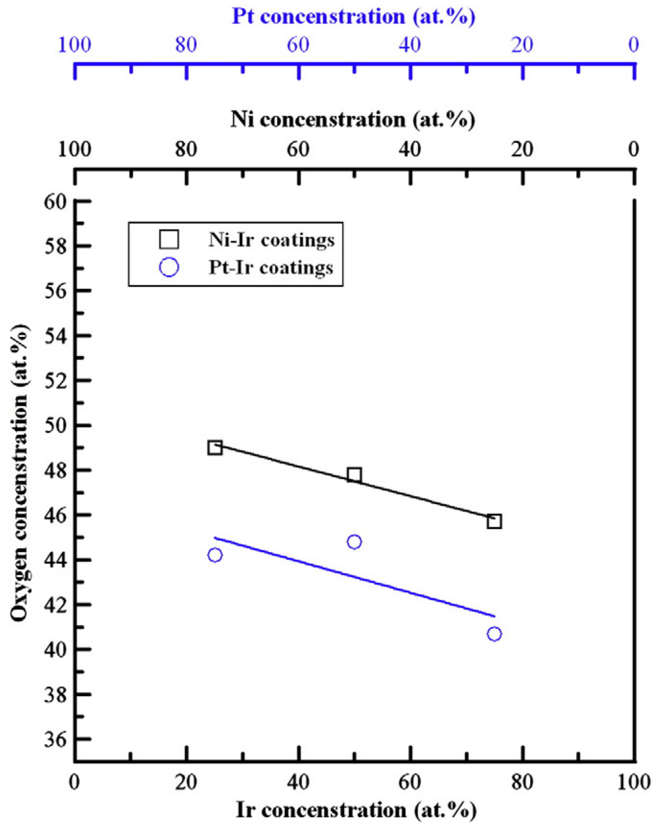


**Fig. 6.** Oxygen concentration of Pt–Ir and Ni–Ir coatings after laser surface treatment.

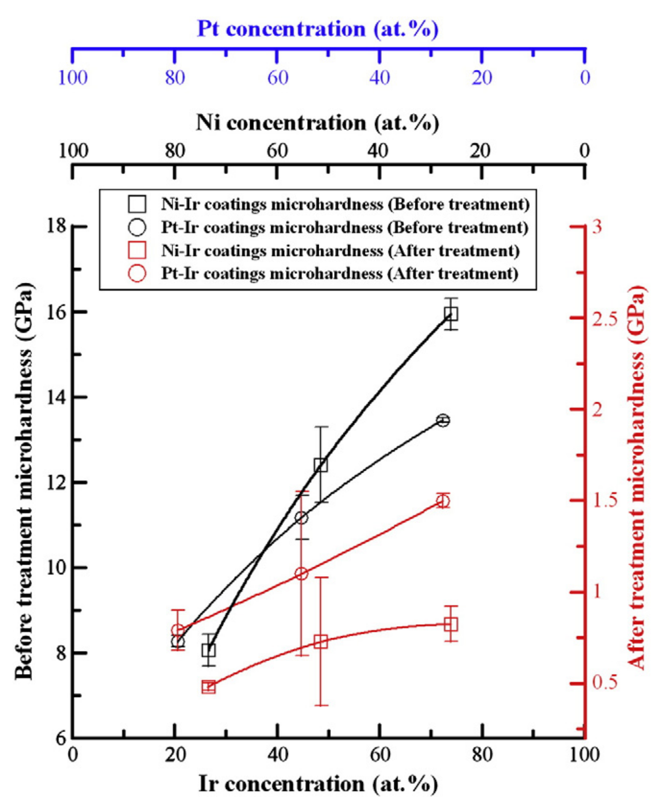


**Fig. 7.** Plot of microhardness testing under different contents of Pt–Ir and Ni–Ir coatings.

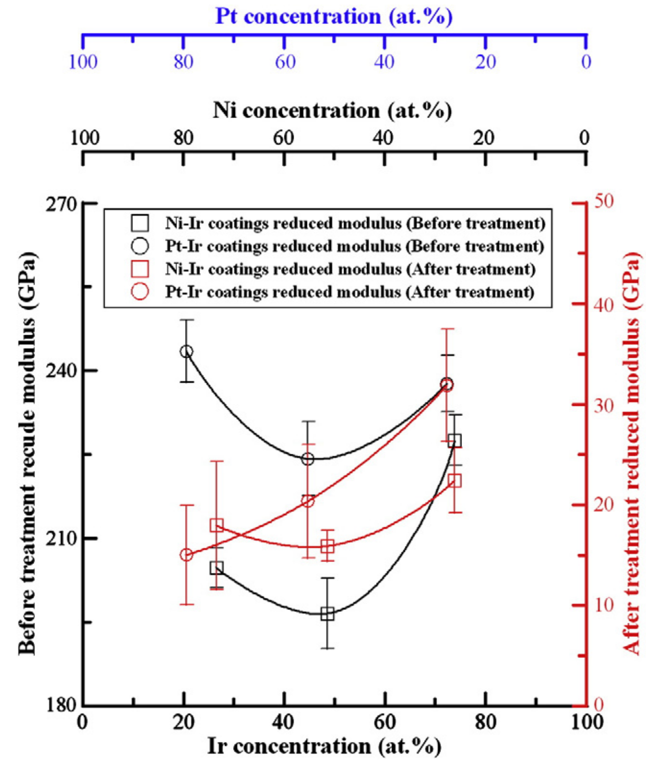


**Fig. 8.** Plot of reduced modulus testing under different contents of Pt–Ir and Ni–Ir coatings.

temperature process. Therefore, we believe that these Ir-alloy coatings operated under the vacuum environment and filled with protective gas are useful in glass molding to avoid the severe surface oxidation and to reduce surface roughness.

## Acknowledgement

The authors would like to thank the National Science Council of the Republic of China, Taiwan for financially supporting this research under contract nos. NSC 98-2221-E-492-008 and NSC 99-2221-E-492-004. Partial support from the optical shop of Instrument Technology Research Center, Taiwan, is also acknowledged.

## References

[1] S.F. Tseng, C.T. Lee, K.C. Huang, D. Chiang, C.Y. Huang, and C.P. Chou, "Mechanical Properties of Pt-Ir and Ni-Ir Binary Alloys for Glass-Molding Dies Coating", *J. Nanosci. Nanotechnol.* 11. (in press: Doi 10.1166/jnn.2011.3502).
[2] C.H. Lin, J.G. Duh, B.S. Yau, Surf. Coat. Technol. 201 (2006) 1316.
[3] L.C. Chang, Y.I. Chen, J.W. Lee, H.Y. Lin, Y.C. Kuo, C.J. Wang, Surf. Coat. Technol. 202 (2007) 967.
[4] Y.I. Chen, L.C. Chang, J.W. Lee, C.H. Lin, Thin Solid Films 518 (2009) 194.
[5] C.T. Wei, H.P.D. Shieh, Jpn. J. Appl. Phys. 45 (2006) 6405.
[6] D. Rosenthal, Weld. J. 20 (1941) 220.
[7] D.H. Kang, K.J. Son, Y.S. Yang, Finite Elem. Anal. Des. 37 (2001) 749.
[8] P. Gordon, B. Balogh, B. Sinkovics, Microelectron. Reliab. 47 (2007) 347.
[9] T.J. McKee, Electron. Technol. 7 (1996) 27.
[10] H.B. Liu, D.P. Wan, D.J. Hu, J. Mater. Process. Technol. 209 (2009) 805.
[11] R.S. Razavi, M. Salehi, M. Monirvaghefi, G.R. Gordani, J. Mater. Process. Technol. 195 (2008) 154.
[12] A. Erdemir, Tribol. Int. 38 (2005) 249.
[13] A. Kovalchenko, O. Ajayi, A. Erdemir, G. Fenske, I. Etsion, Tribol. Int. 38 (2005) 219.
[14] X. Wang, K. Tako, K. Adachi, K. Aizawa, Tribol. Int. 34 (2001) 703.
[15] D.P. Wan, B.K. Chen, Y.M. Shao, S.L. Wang, D.J. Hu, Appl. Surf. Sci. 255 (2008) 3251.
[16] S.F. Tseng, W.T. Hsiao, M.F. Chen, K.C. Huang, S.Y. Hsiao, Y.S. Lin, C.P. Chou, Surface Wettability of Silicon Substrates Enhanced by Laser Ablation, Appl. Phys. A (2010), doi:10.1007/s00339-010-5821-y (Online publication).
[17] Y.C. Chim, X.Z. Ding, X.T. Zeng, S. Zhang, Thin Solid Films 517 (2009) 4845.